Malaysian Journal of Civil Engineering 30(2):217-238 (2018)

APPROPRIATE BASE STIFFNESS OF SMART BASE ISOLATION SYSTEM

Hamed Dadkhah* & Mahsa Noruzvand

Department of Civil Engineering, University of Mohaghegh Ardabili, Ardabil, Iran

*Corresponding Author: *h.dadkhah@uma.ac.ir*

Abstract: In this paper, the effect of base stiffness on the performance of hybrid control system of base isolation system and magnetorheological (MR) damper has been studied and its appropriate base stiffness has been determined. Many researches have been proposed that in the structure controlled by the single base isolation system without MR damper, the base stiffness should be designed such that the fundamental period of isolated structure is almost triple the fundamental period of fixed-base structure. To determine the appropriate base stiffness of hybrid control system, different values have been considered as base stiffness and MR damper has been also employed in two cases of passive form that voltage and dynamical behaviour of MR damper is constant (hybrid base isolation) and semi-active form that MR damper voltage is applied by H2/linear quadratic Gaussian (LQG) and clipped-optimal control algorithms (smart base isolation). For numerical simulation, a three-story shear frame has been subjected to El Centro, Northridge and Tabas earthquakes. Results show that in the structure controlled by the single base isolation system, the peak responses of structure strongly depend on the base stiffness while the sensitivity of peak responses to the base stiffness is lower when the structure is controlled by hybrid base isolation system. According to results, it can be concluded that the peak base drift of hybrid base isolation system reduces with the increase of the base stiffness while this reduction trend is less considerable in the stiffness that are more than the proposed stiffness for the single base isolation system. Hence the proposed stiffness for single base isolation system is the appropriate stiffness for hybrid base isolation system, too. Results also show that under earthquakes considered in this paper, the smart base isolation system is mostly more effective than hybrid base isolation system in mitigating and controlling both root mean square and maximum of structure responses such as base drift, inter-story drift and acceleration.

Keywords: *Base isolation system stiffness, MR damper, clipped-optimal control algorithm, base drift.*

Article history:
Received 19 April 2017
Received in revised form 15 February2018
Accepted 11 April 2018
Published online 30 June 2018

1.0 Introduction

Base isolation system is an effective control system in mitigating the vibration of structure subjected to earthquake. Period elongation of structure and reducing the transmission of seismic force are the purposes of using the base isolation system. Though the period

elongation of structure can reduce structure responses, the base isolation system often experiences high level of drift in the base. Several alternatives could be used for decreasing the base drift such as using high damping rubber (Naeim and Kelly, 1999) and adding supplemental viscous dampers (Constantinou *et al*., 1993; Hwang *et al*., 2010). Though these methods can reduce the base drift, these systems do not have the capability of adapting to different earthquakes. Another method of increasing damping as well as adapting base isolation system to different conditions is adding active control systems (Inaudi and Kelly, 1993; Yang *et al*., 1996) and semi-active control system such as variable orifice damper (Wongprasert and Symans, 2005), variable stiffness system (Narasimhan and Nagarajaiah, 2005) and Magnetorheological (MR) damper to the base isolation system. The results of previous researches indicate the effectiveness of using these supplemental systems in mitigating base drift and adapting to different earthquakes, simultaneously (Ramallo *et al*., 2002; Yoshioka *et al*., 2002).

Because the semi-active base isolation systems need low external power supply during seismic events, these systems have been used more than active system in hybrid with base isolation system. MR damper is one of semi-active control system that has been investigated separately (Dyke *et al*., 1996; Jansen and Dyke, 2000; Jung *et al*., 2003; Moon *et al*., 2011) and in combination with the base isolation system (Yoshioka *et al*., 2002; Bani-Hani and Sheban 2006; Wang and Dyke, 2013; Chen *et al*., 2014; Mohebbi *et al*., 2015) that is called smart base isolation system. Dyke *et al*. (1996) experimentally studied the performance of a fixed-base structure subjected to earthquake excitation while a MR damper had been employed at the first story.

Ramallo *et al*. (2002) experimentally demonstrated the effectiveness of smart base isolation system in reducing the peak response of structure and compared its performance with the passive damper under far-field and near-field earthquake excitations. Sahasrabudhe and Nagarajaiah (2005) experimentally showed the effectiveness of MR damper and base isolation system in controlling structure response under near-field earthquake excitation in a scaled two-story model. Kim *et al*. (2015) employed a smart base isolation system for controlling the micro vibrations of a high-technology facility subjected to train-induced excitation. Gu *et al*. (2016) showed that the smart base isolation system enables the structure to avoid resonant state under earthquake loading. Mohebbi *et al*. (2017) proposed a genetic algorithm-based design approach for the smart base isolation systems.

In previous researches, the performance of smart base isolation system has not been studied completely and the effect of base stiffness on its performance has not been investigated. In the structures controlled by single base isolation system, the base stiffness has been proposed to be selected such that the fundamental period of isolated structure is almost triple the fundamental period of fixed-base structure (Villaverde, 2009). In the structures controlled by smart base isolation system, the performance of control system should be studied for different values of base stiffness to determine the appropriate stiffness and it should be investigated that the proposed stiffness for the single base isolation system is appropriate base stiffness for the smart

base isolation system. Hence in this paper, while different values have been considered as the base stiffness, the performance of smart base isolation system is studied and the appropriate base stiffness of this hybrid control system is determined.

2.0 System Model

Assuming the structure controlled by the smart base isolation system remains in linear region. So the motion equation of structure controlled by smart base isolation system can be written (Dyke *et al*., 1996)

$$M_S\ddot{x} + C_S\dot{x} + K_S x = \Gamma f - M_s \Lambda \ddot{x_g} \tag{1}$$

where $\Gamma = [-1\ 0_i]^T$ indicates the position of MR damper that is installed between ground and base isolation system, f = the force of MR damper, Λ= a vector that all components are unity, x is the vector of the displacements of the structure relative to the ground and M_s, K_s and C_s are mass, stiffness and damping matrices and $\ddot{x}_g$ is the ground acceleration.

The state-space form of the motion equation is given by (Dyke *et al*. 1996)

$$\dot{Z} = AZ + Bf + E\ddot{x_g} \tag{2}$$

$$y = CZ + Df + v \tag{3}$$

where Z is the state vector ($Z=[x\ \dot{x}]^T$), y is the vector of measured outputs, v is the measurement noise vector and A, B, C, D and E are system matrices.

3.0 Smart Base Isolation System Model

Smart base isolation system is a hybrid control system of base isolation and MR damper that MR damper has been installed between ground and base isolation system. In the isolated structure, one degree of freedom is added to dynamical model of structure and MR damper force is applied to this degree of freedom. Parameters of the added degree are m_0, c_0 and k_0 that the base mass, m_0, is chosen almost equal to the floor mass. The base damping, c_0, is chosen such that the damping ratio of the low damping base isolation system is almost 2% of critical damping of isolated mode (Naeim and Kelly, 1999). In the isolated mode, it is assumed that the superstructure of isolated structure is rigid and the controlled structure is considered as a single degree of freedom system with the natural frequency and damping ratio of the base isolation system. The period of the isolated mode is computed by (Bisch *et al*., 2012):

$$T_{iso} = 2\pi\sqrt{\frac{m_0 + \sum_{i=1}^{n} m_i}{k_0}} \tag{4}$$

where m_i is the mass of the i^{th} story, n is the number of stories and k_0 the stiffness of base isolation system. Many researches have been proposed that in the structure controlled by the single base isolation system without MR damper, k_0 should be designed such that T_{iso} is almost triple the fundamental period of fixed-base structure (Naeim and Kelly, 1999; Villaverde, 2009; Bisch *et al*., 2012). In this paper, different values are considered for the base stiffness of smart base isolation system to obtain the appropriate stiffness. The base damping, c_0, is determined by (Naeim and Kelly, 1999):

$$c_0 = \xi c_{cr} = 0.02 \times 2\sqrt{k_0(m_0 + \sum_{i=1}^{n} m_i)} \tag{5}$$

where ξ is the damping ratio and c_{cr} is the critical damping. Because MR damper is a semi-active control system that can be adapted to different conditions by changing the MR damper voltage, the smart base isolation system can be also adapted to different conditions. The simple mechanical idealization of the MR damper is depicted in Figure 1.

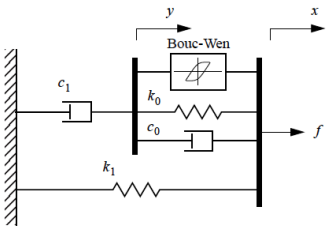

Figure 1: Simple mechanical model of the MR damper

The force applied by this model is given as (Dyke *et al*. 1996):

$$f = az + c_0(\dot{x} - \dot{y}) + k_0(x - y) + k_1(x - x_0) \tag{6}$$

or equivalently

$$f = c_1\dot{y} + k_1(x - x_0) \tag{7}$$

$$\dot{z} = -\gamma|\dot{x} - \dot{y}||z|z|^{n-1} - \beta(\dot{x} - \dot{y})|z|^n + A(\dot{x} - \dot{y}) \tag{8}$$

$$\dot{y} = \frac{1}{c_1 + c_0}\{az + c_0\dot{x} + k_0(x - y)\} \tag{9}$$

where k_1, c_0 and c_1 represent the accumulator stiffness, the viscous damping and dashpot, respectively. Also k_0 is present to control the stiffness at the large velocities, x_0 is the initial displacement of spring k_1 and the parameters γ, β and A are the parameters which used to define the shape of hysteresis loops. The dynamical behavior of MR damper depends on its voltage. Spencer *et al.* (1997) have suggested the following equations to determine the parameters of MR damper dynamic model based on the applied voltage:

$$a = a(u) = a_a + a_b u \tag{10a}$$

$$c_1 = c_1(u) = c_{1a} + c_{1b} u \tag{10b}$$

$$c_0 = c_0(u) = c_{0a} + c_{0b} u \tag{10c}$$

where u is given as the output of a first-order filter given by:

$$\dot{u} = -\eta(u - V) \tag{11}$$

V is the voltage that currents in MR damper and η is constant modulus with dimension Sec^{-1}.

4.0 Control Algorithm

In this paper, the desired control force has been calculated by H_2/LQG (Linear Quadratic Gaussian) control algorithm (Dyke *et al.* 1996). For designing of controller, $\ddot{x}_g$ is taken to be a stationary white noise. The regulated outputs are minimized using the following cost function:

$$J = \lim_{\tau \to \infty} \frac{1}{\tau} E\left[\int_0^{\tau} \left(\boldsymbol{z}^T(t)\boldsymbol{Q}\boldsymbol{z}(t) + r{f_c}^2\right)dt\right] \tag{12}$$

where Q and r are the weighting matrix and parameter. The elements of Q are determined according to the main purpose of control system design.

The desired control force is given as follows:

$$f_c = -k_c \bar{z} \tag{13}$$

$$\dot{\bar{z}} = A\bar{z} + Bf + L(y - C\bar{z} - Df) \tag{14}$$

k_c is the gain matrix for Linear Quadratic Regulator (LQR) and L is the gain matrix for state estimator which is determined as:

$$k_c = \frac{\acute{B}P}{r} \tag{15}$$

$$L = (CS)' \tag{16}$$

where P and S are the solution of the algebraic Ricatti equation given by Dyke *et al*. (1996):

$$PA + \acute{A}P - P\acute{B}BP/r + Q = 0 \tag{17}$$

$$S\acute{A} + AS - S\acute{C}CS + \gamma E\acute{E} = 0 \tag{18}$$

The MR damper force depends on the local response of structure in the place that MR damper has been installed and applied voltage. Because only the voltage can be directly changed, it should be changed such that the MR damper force is approached to the desired control force calculated by H_2/LQG control algorithm. In this study the clipped-optimal control is used to apply the voltage of MR damper where the voltage is determined as (Dyke *et al*., 1996):

$$V = V_{max} H\{(f_c - f)f\} \tag{19}$$

V_{max} is the maximum voltage that can be applied to MR damper, and $H\{.\}$ is the Heaviside step function (Dyke *et al*., 1996). In the clipped-optimal control when the force produced by MR damper is smaller than the desired optimal force and two forces are the same sign, the voltage applied to MR damper is increased to the maximum level. Otherwise, the voltage applied is set to zero.

A block diagram of the clipped-optimal control and a block diagram of the semi-active control system have been shown in Figures 2 and 3.

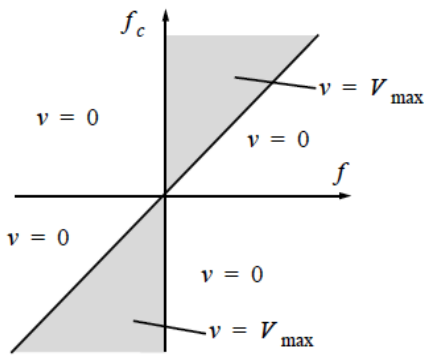

Figure 2: Diagram of clipped-optimal control system

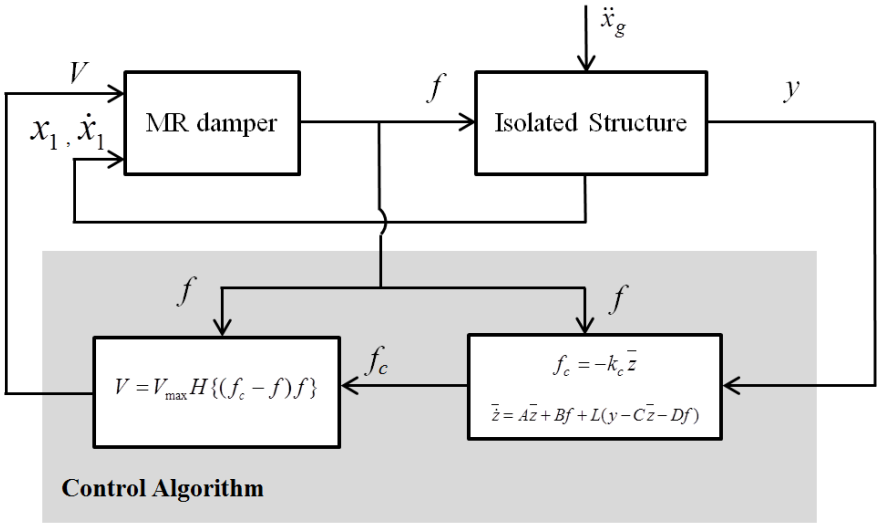

Figure 3: Diagram of semi-active control system

5.0 Numerical Example

Dyke *et al*. (1996) experimentally studied the performance of a scaled model of three-story shear frame in the fixed-base case while a MR damper had been employed at the first story. For numerical analysis, the performance of this structure is investigated in the isolated case while the same MR damper has been installed between ground and base isolation system. In the isolated case, one degree of freedom is added to dynamical model of the structure at the base. The dynamical models of structure controlled by smart base isolation system have been shown in Figure 4.

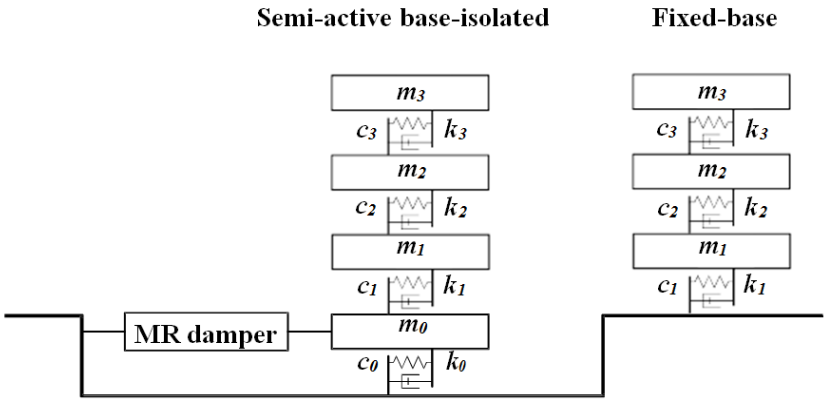

Figure 4: Model of the structure

The dynamic properties of fixed-base structure have been reported in Table 1. The natural periods of vibration modes of considered structure are equal to 0.18, 0.06 and 0.04 (s). In the isolated model, the superstructure properties on the base isolation system are the same as fixed-base structure. The dynamic parameters of base isolation system are m_0, c_0 and k_0. The base mass, m_0, is chosen 98.3 (kg) and different values have been considered for the base stiffness, k_0. Because the base isolation system has been considered in combination with MR damper, the utilization of high damping base isolation system is not essential to mitigate base drift. Therefore in this paper, a low damping base isolation system, which the damping ratio is almost 2% of critical damping of isolated mode (Naeim and Kelly, 1999), has been considered as base isolation system.

Table 1: Parameters of fixed-base structure (Dyke *et al*. 1996)

Story	*Floor Masses (kg)*	*Stiffness Coefficients* $\times 10^5$ *(N/m)*	*Damping Coefficients (N.s/m)*
1	98.3	5.16	125
2	98.3	6.84	50
3	98.3	6.84	50

For numerical simulations, a program has been developed using the MATLAB software. To verify the result of the numerical analysis, the output of the current research has been compared with the results of the experimental study conducted by Dyke *et al*. (1996) and reported in Table 2. It is clear that an acceptable adaption has been achieved between the results.

Table 2: Verifying the written code in Matlab program

Control Strategy	*Uncontrolled Structure*		*Clipped-Optimal Control*	
	Dyke et al. (1996)	*Present Research*	*Dyke et al. (1996)*	*Present Research*
x_1	0.538	0.542	0.114	0.113
x_2	0.820	0.836	0.185	0.190
x_3	0.962	0.973	0.212	0.215
(cm)				
$\ddot{x}_1$	856	848	696	688
$\ddot{x}_2$	1030	1032	739	698
$\ddot{x}_3$	1400	1413	703	682
(cm/s^2)				
$f(N)$	-		941	923

By defining *y* as a vector which includes the absolute accelerations of the base isolation and the structure floors and the displacement of base isolation (i.e. $y=[\ddot{x}_b \ddot{x}_1 \ddot{x}_2 \ddot{x}_3 x_b]^T$), the system matrices of Eq.s (2) and (3) can be written as:

$$A=\begin{bmatrix} 0_{4\times4} & I_{4\times4} \\ -M_S^{-1}K_S & -M_S^{-1}C_S \end{bmatrix}, \quad (20)$$

$$B=\begin{bmatrix} 0_{4\times1} \\ M_S^{-1}\Gamma \end{bmatrix},\ E=\begin{bmatrix} 0_{4\times1} \\ \Lambda_{4\times1} \end{bmatrix}, \quad (21)$$

$$C=\begin{bmatrix} -M_S^{-1}K_S & -M_S^{-1}C_S \\ 1\,0\,0\,0 & 0\,0\,0\,0 \end{bmatrix}, \quad (22)$$

$$D=\begin{bmatrix} M_S^{-1}\Gamma \\ 0 \end{bmatrix} \quad (23)$$

M_s, K_s and C_s are mass, stiffness and damping matrices defined in Eq. (1).

The selected MR damper is a damper with capacity and maximum voltage of 3000 (*N*) and 2.25 (*V*), respectively which has been employed by Dyke *et al*. (1996) for controlling a fixed-based structure. In this paper, this MR damper is considered as the supplemental damper of base isolation system and its dynamical parameters are given in Table 3. The selected MR damper is a sample which has been efficient in controlling the responses and the base drift of the considered structure. In practical applications, the capacity and dynamical parameters of MR damper could be designed in such a way that the responses and base drift of the isolated structure fall in a desired level defined according to the design criteria. The control system performance is evaluated under the El Centro (PGA=0.35g, 1940), Northridge (PGA=0.58g, 1994) and Tabas (PGA=0.85g, 1978) earthquakes. Because the considered structure is a scaled model, all considered earthquake records have been reproduced at five times the recorded rate.

Table 3: Parameters of MR damper (Dyke *et al*. 1996)

Parameter	*Value*	*Parameter*	*Value*
c_{0a}	21 *N.sec/cm*	a_a	140 *N/cm*
c_{0b}	3.5 *N.sec/cm.V*	a_b	695 *N/cm.V*
k_0	46.9 *N/cm*	γ	363 cm^{-2}
c_{1a}	283 *N.sec/cm*	β	363 cm^{-2}
c_{1b}	2.95 *N.sec/cm.V*	A	301
k_1	5 *N/cm*	n	2
x_0	14.3 *cm*	η	190 sec^{-1}

In this paper, the studied numerical simulations can be classified into three cases as follows:

Case (a): In this case, the base stiffness is considered equal to stiffness proposed for the single base isolation system and the MR damper is employed in the passive form with the constant voltage.

Case (b): different values have been considered for the base stiffness of isolation system in hybrid with passive MR damper.

Case (c): The MR damper is used in the semi-active form and the base stiffness has been chosen based on the results of *Case (b)*.

5.1 Hybrid Base Isolation with the Base Stiffness Proposed for Single Base Isolation

For designing single base isolation system, the base stiffness has been proposed to be selected such that the fundamental period of the isolated structure is almost triple the fundamental period of the fixed-base structure (Villaverde, 2009). Based on this design approach, the fundamental period of the fixed-base structure (0.18s) and Eq. (4), k_0 is selected equal to 56 (*kN/m*).

In this case, the MR damper acts in passive form with constant voltage during earthquake. The control system performance could be evaluated for each voltage which Yoshioka *et al*. (2002) has been presented the effect of constant voltage on the responses of isolated structure. Yoshioka *et al*. (2002) demonstrated that the greatest and least values of peak base drift are obtained for constant voltages of 0 and maximum. In this paper, for example, the maximum response of uncontrolled and controlled structures has been reported in Tables 4, 5 and 6 for voltages of 0, 1.5 and 2.25 (*V*) when the structure is subjected to the El Centro, Northridge and Tabas earthquakes. x_b, d_b and $\ddot{x}_b$ are displacement, drift and absolute acceleration of the base isolation. x_i, d_i and $\ddot{x}_i$ are displacement, inter-story drift (x_i-x_{i-1}) and absolute acceleration of the i^{th} floor and f is MR damper force.

As shown in Tables 4, 5 and 6, the maximum response of fixed-base structure has been reduced by isolating structure which in this case study, about 78 and 83% reduction respectively in the average of maximum drifts and accelerations under considered earthquakes have been achieved. Though using single base isolation system decreases the structure response effectively, the peak base drift is significantly high for a scaled structure with the floor masses of 98.3 (kg). The peak base drift can be decreased by using MR damper that has been installed between base isolation system and ground. According to results, it is clear that adding passive MR damper mitigates the peak base drift, significantly and more reduction in the peak base drift can be obtained by increasing of MR damper voltage which in this case for constant voltages of 0, 1.5 and 2.25 (*V*), the average of maximum base drifts have been reduced about 68, 78 and 82% respectively. Though the peak superstructure response of structure controlled by hybrid base isolation system is more than single base isolation system

in most cases, comparing the results of fixed-base structure and structure controlled by hybrid base isolation shows the maximum structure response when using hybrid base isolation system is less than fixed-base structure. Hence, hybrid base isolation system is an effective control system in reducing both the base drift and the structure response.

Table 4: Peak response of uncontrolled and controlled structures under the El Centro earthquake

Control Strategy	*Fixed Base*	*Low Damping Base Isolation*	*Passive Form (voltage=0)*	*Passive Form (voltage=1.5)*	*Passive Form (voltage=2.25)*
x_b	-	1.27	0.44	0.20	0.19
x_1	0.54	1.37	0.48	0.30	0.29
x_2	0.83	1.42	0.50	0.35	0.35
x_3 (cm)	0.97	1.45	0.51	0.40	0.40
d_b	-	1.27	0.44	0.20	0.19
d_1	0.54	0.11	0.06	0.15	0.15
d_2	0.32	0.05	0.04	0.11	0.11
d_3 (cm)	0.20	0.03	0.03	0.07	0.07
$\ddot{x}_b$	-	199	226	285	280
$\ddot{x}_1$	848	197	175	375	408
$\ddot{x}_2$	1032	197	150	323	329
$\ddot{x}_3$ (cm/s^2)	1413	217	207	474	477
$f(N)$	-	-	274	835	878

Table 5: Peak response of uncontrolled and controlled structures under the Northridge earthquake

Control Strategy	*Fixed Base*	*Low Damping Base Isolation*	*Passive Form (voltage=0)*	*Passive Form (voltage=1.5)*	*Passive Form (voltage=2.25)*
x_b	-	1.37	0.44	0.39	0.31
x_1	0.59	1.48	0.51	0.50	0.48
x_2	0.85	1.55	0.56	0.55	0.55
x_3	0.99	1.59	0.59	0.60	0.59
(cm)					
d_b	-	1.37	0.34	0.39	0.31
d_1	0.59	0.13	0.09	0.25	0.31
d_2	0.33	0.07	0.04	0.15	0.18
d_3	0.28	0.04	0.06	0.11	0.15
(cm)					
$\ddot{x}_b$	-	241	389	692	785
$\ddot{x}_1$	1527	232	408	806	897
$\ddot{x}_2$	1385	258	261	487	719
$\ddot{x}_3$	1950	282	401	783	1023
(cm/s^2)					
$f(N)$	-	-	532	935	1243

Table 6: Peak response of uncontrolled and controlled structures under the Tabas earthquake

Control Strategy	*Fixed Base*	*Low Damping Base Isolation*	*Passive Form (voltage=0)*	*Passive Form (voltage=1.5)*	*Passive Form (voltage=2.25)*
x_b	-	2.45	0.72	0.52	0.44
x_1	0.93	2.65	0.79	0.61	0.60
x_2	1.47	2.75	0.84	0.70	0.65
x_3	1.73	2.81	0.88	0.77	0.70
(cm)					
d_b	-	2.45	0.72	0.52	0.44
d_1	0.93	0.21	0.13	0.27	0.30
d_2	0.53	0.11	0.08	0.15	0.15
d_3	0.32	0.07	0.07	0.12	0.12
(cm)					
$\ddot{x}_b$	-	450	654	926	848
$\ddot{x}_1$	1409	405	383	758	854
$\ddot{x}_2$	1942	392	344	623	647
$\ddot{x}_3$	2202	461	458	857	855
(cm/s^2)					
$f(N)$	-	-	1012	1400	1409

5.2 Base Stiffness Effect on the Hybrid Base Isolation system Performance

In previous researches, it can be seen that when the control algorithm of smart base isolation system is designed with the objective of minimizing the peak base drift, smart base isolation system works almost the same as hybrid base isolation system with the constant maximum voltage (Mohebbi *et al*., 2017). So, the appropriate base stiffness of hybrid base isolation system can be considered as the suitable base stiffness for smart base isolation system. In this section, the performance of hybrid base isolation system is investigated for different values of base stiffness to determine the appropriate base stiffness of this hybrid control system. Also, it is evaluated that the proposed stiffness for single base isolation system can be considered as an appropriate base stiffness for hybrid base isolation system. The peak structure response and base drift of controlled structure have been shown for different values of base stiffness in Figure 5.

As shown in Figure 5 in structure controlled by single base isolation system, the peak structure responses and peak base drift strongly depend on the base stiffness while the sensitivity of peak responses to the base stiffness is lower when the structure is controlled by hybrid base isolation system. According to results shown in Figure 5(a), it can be concluded that when the applied voltage on hybrid base isolation system is close to the maximum voltage of MR damper, the increase of the base stiffness reduces the peak base drift of controlled structure while at the stiffnesses above about the stiffness proposed for single base isolation (56 *kN/m*), the decrease of peak base drift is insignificant. For example under El Centro earthquake, it can be seen that at the stiffnesses above 50 (*kN/m*), the peak base drift is almost constant. On the other hand, it can be seen from Figures 5(b) and 5(c) that the peak inter-story drift and peak acceleration of structure mostly increase by increasing the base stiffness. Hence, it can be concluded that the proposed base stiffness for single base isolation system can be considered as appropriate stiffness for hybrid base isolation system. The results show that when MR damper operates with low voltage (0v) and the responses of structure at the base (the displacement and velocity of damper) is insignificant, the increase of peak base drift is possible with an increase in the base stiffness because the applied force by MR damper is not sufficient to control the resonant of isolated structure. For example, it can be seen from Figure 5(a) that under Northridge earthquake and voltage of 0(v), the peak base drift increases from the base stiffness of 50 up to 300 (*kN/m*).

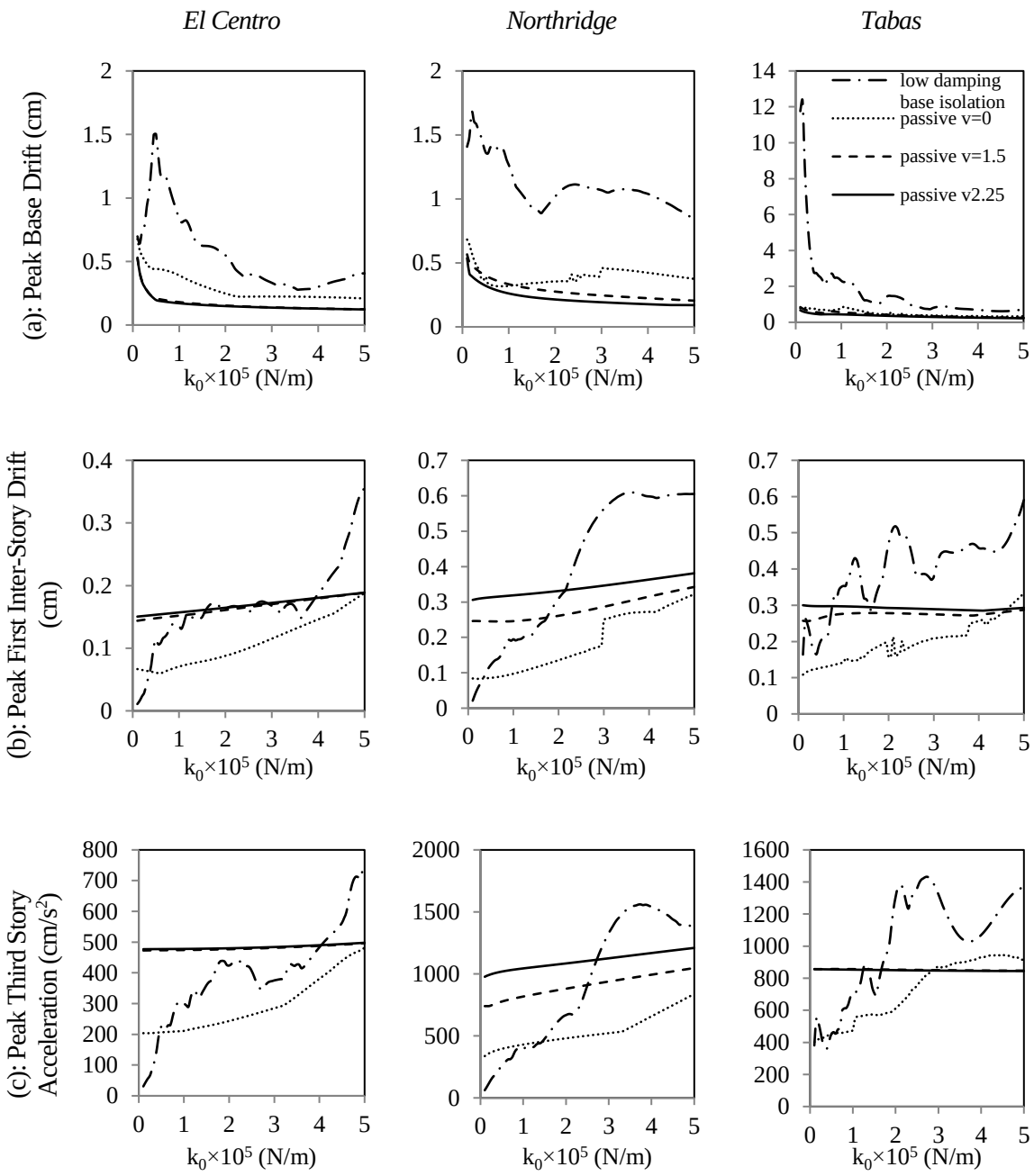

Figure 5: Effect of base isolation system stiffness on the peak response of structure under different earthquakes

5.3 Smart Base Isolation System

In this section, the clipped-optimal control algorithm is used to apply the voltage of the MR damper in each time step. The operation of this control algorithm depends on the desired control force calculated in each time step while this force strongly depends on weighting parameters defined in the H_2/LQG control algorithm. In Eq. (12), all elements of Q are zero, except for $Q_{(1,1)}$=1 because MR damper has been added to base isolation system to control base drift. Dadkhah and Noruzvand (2017) evaluated the performance of smart base isolation system for different sets of Q and showed that smart base isolation system is efficient in controlling base drift when Q is related to the displacement of structure. To determine weighting parameter, r, the maximum response of structure subjected to El Centro earthquake has been shown in Figure 6 for different values of r. As shown in Figure 6, with decrease of r, the peak base drift reduces while the peak acceleration and inter-story drift increase. Because in this paper the design objective has been considered controlling the base drift, the appropriate value of weighting parameter is selected equal to 9.12×10^{-12}.

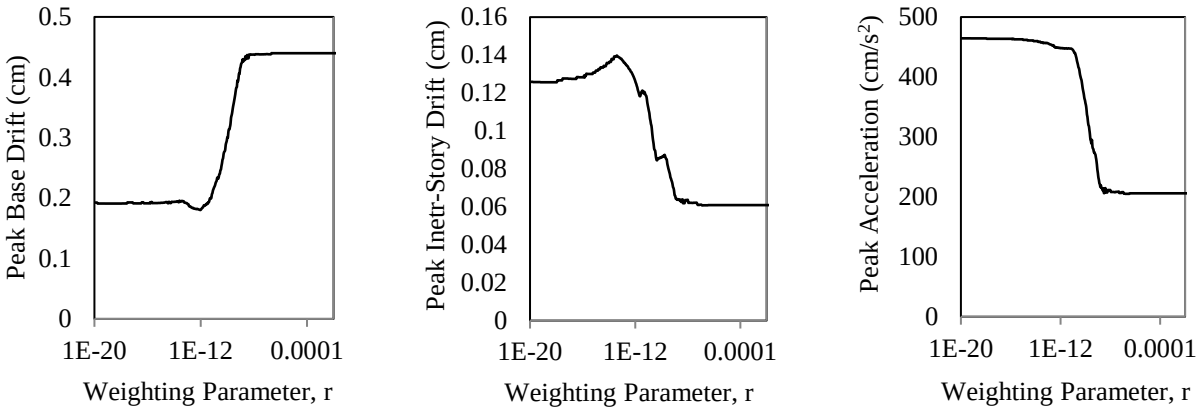

(a): Peak base drift (b): Peak inter-story drift (c): Peak third story acceleration

Figure 6: The peak responses of structure for different values of r under El Centro earthquake

The maximum response of controlled structures by designed control system has been reported in Table 7 when the structure has been subjected to the El Centro earthquake. In addition to the peak responses, for better evaluation of performance of smart base isolation system and its comparison with hybrid base isolation system (passive form), the root-mean-square (RMS) of responses has been determined by using Eq. (24).

$$RMS_z = \sqrt{\frac{1}{n}(z_1^2 + z_2^2 + \cdots + z_n^2)} \tag{24}$$

As shown in Table 7, adding the semi-active MR damper can reduce the peak base drift more than passive MR damper. The RMS of base drift of structure controlled by smart base isolation system is also 30% less than hybrid base isolation system. Figure 7 shows time histories of the base drift, first story drift and third story acceleration for different control systems and Figures 8 and 9 show voltage and force of MR damper.

Table 7: Response of controlled structures under the El Centro earthquake

Control Strategy	*Low Damping Base Isolation*		*Hybrid Base Isolation (passive v=2.25)*		*Smart Base Isolation*	
	Peak	*RMS*	*Peak*	*RMS*	*Peak*	*RMS*
x_b	1.50	0.78	0.20	0.13	0.18	0.09
x_1	1.61	0.84	0.30	0.13	0.26	0.10
x_2	1.67	0.87	0.35	0.14	0.31	0.11
x_3	1.70	0.88	0.40	0.15	0.33	0.11
(cm)						
d_b	1.50	0.78	0.20	0.13	0.18	0.09
d_1	0.11	0.06	0.15	0.04	0.13	0.03
d_2	0.06	0.03	0.11	0.02	0.08	0.02
d_3	0.03	0.02	0.07	0.01	0.06	0.01
(cm)						
$\ddot{x}_b$	203	98	280	54	562	71
$\ddot{x}_1$	199	103	407	71	422	74
$\ddot{x}_2$	214	107	328	78	395	69
$\ddot{x}_3$	225	110	477	100	448	84
(cm/s^2)						
$f(N)$	0	-	876	-	652	-

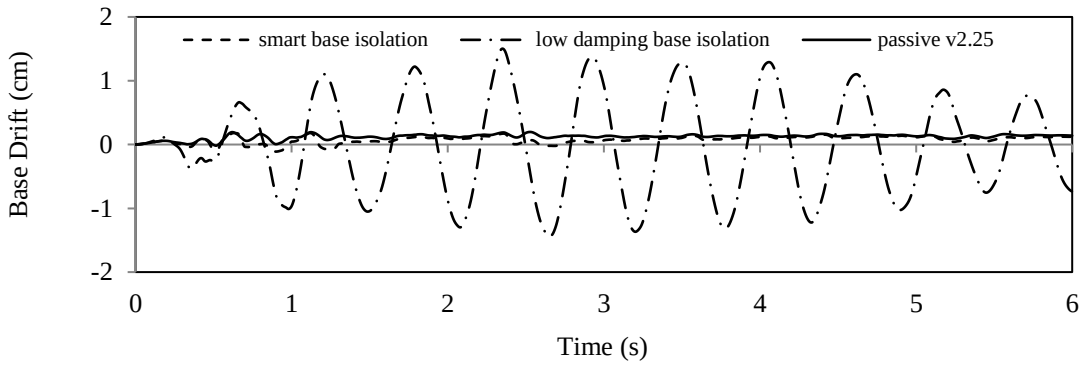

(a): Base drift

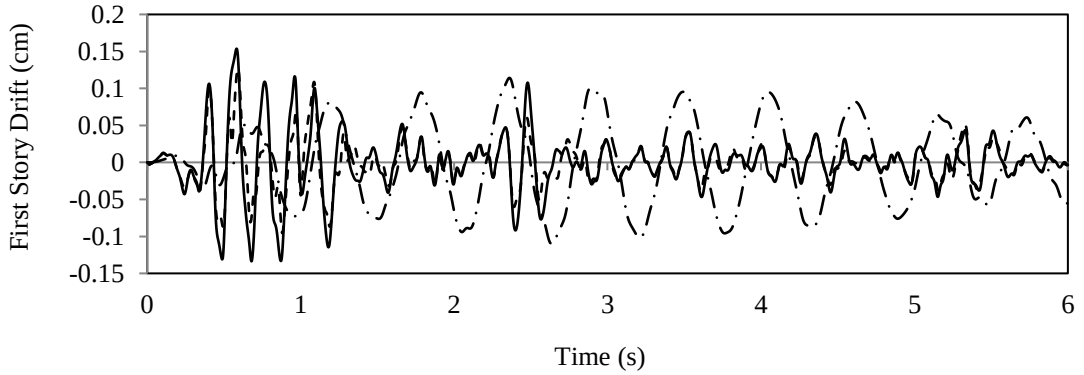

(b): First story drift

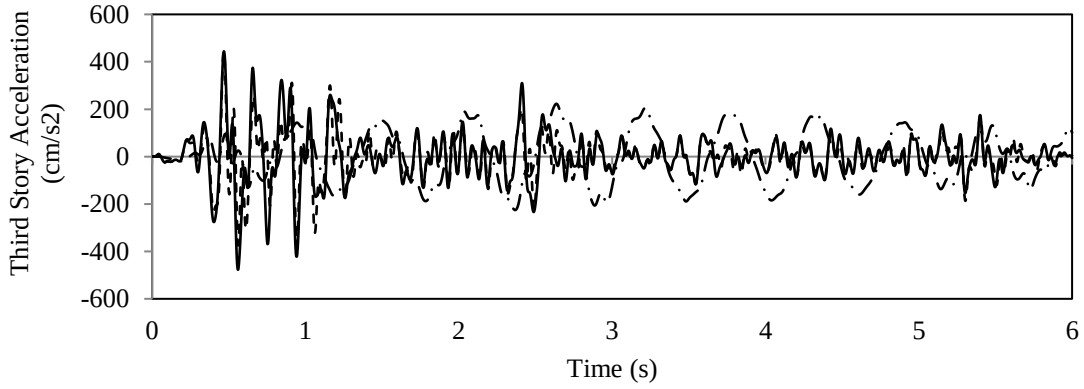

(c): Third story acceleration

Figure 7: Comparison of the peak responses of structure by using different control system

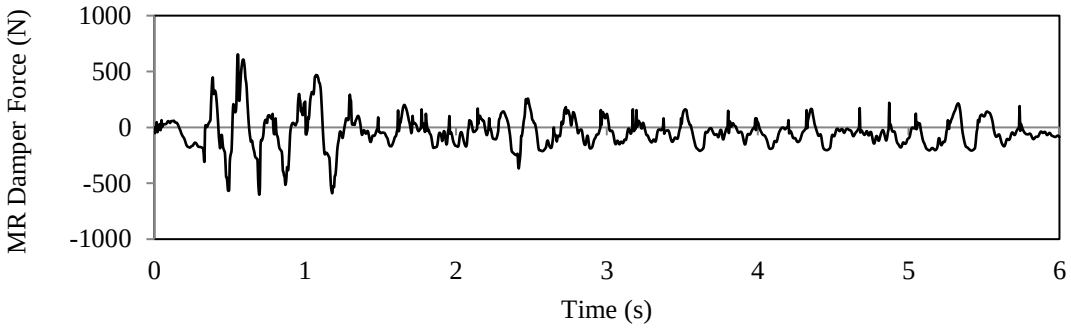

Figure 8: MR damper force

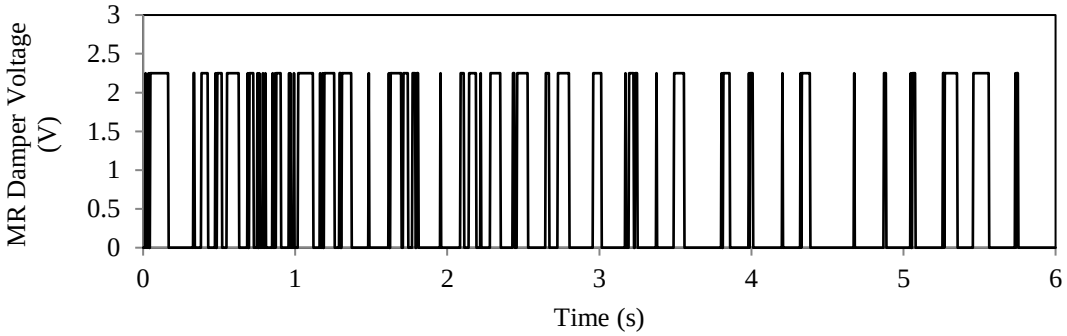

Figure 9: Applied voltage on the MR damper

To evaluate the performance of designed smart base isolation system under other earthquake records, the structure responses have been presented in Tables 8 and 9 under Northridge and Tabas earthquakes. According to the results, it is clear that under Northridge earthquake, the smart base isolation system works more effective than hybrid base isolation system in mitigating the maximum and RMS of responses. Although under Tabas earthquake, the peak base drift of structure controlled by smart base isolation system is more than hybrid base isolation system, it is 80% less than structure controlled by single base isolation system. Hence smart base isolation system designed for El Centro earthquake has appropriate performance under other earthquakes.

Table 8: Response of controlled structures under the Northridge earthquake

Control Strategy	*Low Damping Base Isolation*		*Hybrid Base Isolation (passive v=2.25)*		*Smart Base Isolation*	
	Peak	*RMS*	*Peak*	*RMS*	*Peak*	*RMS*
x_b	1.36	0.48	0.32	0.13	0.28	0.11
x_1	1.48	0.52	0.49	0.14	0.40	0.13
x_2	1.55	0.54	0.55	0.15	0.50	0.14
x_3	1.59	0.55	0.60	0.16	0.60	0.14
(cm)						
d_b	1.36	0.48	0.32	0.13	0.28	0.11
d_1	0.12	0.04	0.31	0.04	0.18	0.04
d_2	0.07	0.02	0.18	0.03	0.12	0.02
d_3	0.04	0.01	0.15	0.02	0.10	0.02
(cm)						
$\ddot{x}_b$	227	67	780	87	652	95
$\ddot{x}_1$	202	66	896	132	671	114
$\ddot{x}_2$	242	68	715	93	448	86
$\ddot{x}_3$	259	73	1019	139	679	119
(cm/s^2)						
$f(N)$	0	-	1241	-	1044	-

Table 9: Response of controlled structures under the Tabas earthquake

Control Strategy	*Low damping Base Isolation*		*Hybrid Base Isolation (passive v=2.25)*		*Smart Base Isolation*	
	Peak	*RMS*	*Peak*	*RMS*	*Peak*	*RMS*
x_b	2.60	0.92	0.45	0.16	0.51	0.14
x_1	2.80	0.99	0.59	0.18	0.60	0.17
x_2	2.90	1.02	0.64	0.20	0.70	0.19
x_3	2.97	1.04	0.71	0.22	0.78	0.21
(cm)						
d_b	2.60	0.92	0.45	0.16	0.51	0.14
d_1	0.20	0.07	0.30	0.07	0.25	0.06
d_2	0.11	0.03	0.15	0.04	0.13	0.03
d_3	0.07	0.02	0.12	0.03	0.10	0.02
(cm)						
$\ddot{x}_b$	405	120	848	144	805	150
$\ddot{x}_1$	373	122	854	148	584	145
$\ddot{x}_2$	379	126	646	161	589	134
$\ddot{x}_3$	452	132	855	197	720	164
(cm/s^2)						
$f(N)$	0	-	1413	-	1278	-

6.0 Conclusion

In this paper, the effect of base isolation system stiffness on the performance of hybrid control system of base isolation and MR damper has been studied and the appropriate base stiffness of this hybrid control system has been determined. Different values have been considered for base isolation stiffness and MR damper has been also used in the forms of passive (hybrid base isolation) and semi-active (smart base isolation). In the passive form, voltage and dynamical behaviour of MR damper is constant during loading while in the semi-active form, the voltage of MR damper is applied by the H_2/ LQG and clipped-optimal control algorithms in each time step. For numerical simulation, a three-story frame has been subjected to El Centro, Northridge and Tabas earthquakes. Results show that in the structure controlled by single base isolation system, the peak response of structure such as the base drift, inter-story drift and acceleration strongly depends on the base stiffness while the sensitivity of peak responses to the base stiffness is lower when the structure is controlled by hybrid base isolation system.

The performance of hybrid control system shows that the peak base drift reduces with the increase of the base stiffness while at the stiffnesses above about the stiffness proposed for single base isolation, the decrease of peak base drift is insignificant. On the other hand, the results show that the peak inter-story drift and peak acceleration of structure mostly increase by increasing the base stiffness. Hence the base stiffness proposed for single base isolation system can be considered as the appropriate base stiffness for hybrid control system. Results also show that adding semi-active MR damper effectively reduces the peak base drift, inter-story drift and acceleration of structure that in the case study, the average of peak base drift, inter-story drift and acceleration under considered earthquakes has been reduced about 82, 73 and 63%, respectively. Comparing the performance of smart and hybrid base isolation systems shows that under most earthquakes, smart base isolation system is more efficient in mitigating the peak base drift. Although under some earthquake, hybrid base isolation system is more efficient in mitigating the peak base drift, the RMS of base drift and responses of structure controlled by smart base isolation system is less than hybrid base isolation system. Hence, smart base isolation system acts more effective than hybrid base isolation system on controlling structure response.

References

Bani-Hani, K.A., and Sheban, M.A. (2006) Semi-active neuro-control for base-isolation system using magnetorheological dampers. *Earthquake Engineering and Structural Dynamics*, 35: 1119-1144.

Bisch, P., Carvalho, E., Degee, H., and *et al*. (2012) Eurocode 8: seismic design of buildings worked examples. Luxembourg: JRC technical report, Publications Office of the European Union/Joint Research Centre.

Chen, P.C., Tsai, K.C., and Lin, P.Y. (2014) Real-time hybrid testing of a smart base isolation system. *Earthquake Engineering and Structural Dynamics*, 43: 139-158.

Constantinou, M.C., Symans, M.D., Tsopelas, P., and Taylor, D.P. (1993) Fluid dampers for application of seismic energy dissipation and seismic isolation. *Proceeding of ATC-17-1 Seminar on Seismic Isolation, Passive Energy Dissipation and Active Control*.

Dadkhah, H., and Noruzvand, M. (2017) Optimal Response-Related Weighting Matrices to Control Semi-Active Base Isolation Systems. *Slovak Journal of Civil Engineering*, 25: 24-32.

Dyke, S.J., Spencer, B.F., Sain, M.K., and Carlson, J.D. (1996) Modeling and control of Magnetorheological dampers for seismic response reduction. *Smart Materials and Structures*, 5: 565-575.

Gu, X., Li, J., Li, Y., and Askari, M. (2016) Frequency control of smart base isolation system employing a novel adaptive magneto-rheological elastomer base isolator. *Journal of Intelligent Material Systems and Structures*, 27: 849-858.

Hwang, J.S., Hung, C.F., Huang, Y.N., and Wang, S.J. (2010) Design force transmitted by isolation system composed of lead-rubber bearing and viscous dampers. *International Journal of Structural Stability and Dynamics*, 10: 287-298.

Inaudi, J.A., and Kelly, J.M. (1993) Hybrid isolation systems for equipment protection. *Earthquake Engineering and Structural Dynamics*, 22: 297-313.

Jansen, L.M., and Dyke, S.J. (2000) Semi-active control strategies for MR damper: A comparative study. *Journal of Engineering Mechanics*, 126: 795-803.

Jung, H.J., Spencer, B.F., and Lee, I.W. (2003) Control of seismically excited cable-stayed bridge employing magnetorheological fluid dampers. *Journal of Structural Engineering*, 129: 873-883.

Kim , H.S., Chang, S., and Kang, J.W. (2015) Evaluation of microvibration control performance of a smart base isolation system. *International Journal of Steel Structures*, 15: 1011-1020.

Mohebbi, M., and Dadkhah, H. (2017) Multi-objective semi-active base isolation system. *International Journal of Optimization in Civil Engineering*, 7: 319-338.

Mohebbi, M., Dadkhah, H., and Dabbagh, H.R. (2017) A genetic algorithm-based design approach for smart base isolation systems. *Journal of Intelligent Material Systems and Structures*, doi: 10.1177/1045389X17733058.

Mohebbi, M., Dadkhah, H., and Shakeri, K. (2015) Optimal hybrid base isolation and MR damper. *International Journal of Optimization in Civil Engineering*, 5: 493-509.

Moon, S.J., Huh, Y.C., Jung, H.J., Jang, D.D., and Lee, H.J. (2011) Sub-optimal design procedure of valve-mode magnetorheological fluid dampers for structural control. *KSCE Journal of Civil Engineering*, 15: 867-873.

Naeim, F. and Kelly, J.M. (1999) Design of seismic isolated structure: from theory to practice. London: Wiley.

Narasinhan, S., and Nagarajaiah, S. (2005) A STFT semi active controller for base isolated buildings with variable stiffness isolation systems. *Engineering Structures*, 27: 514-523.

Ramallo, J.C., Johnson, E.A., and Spencer, B.F. (2002) Smart base isolation systems. *Journal of Engineering Mechanics*, 128: 1088-1099.

Sahasrabudhe, S., and Nagarajaiah, S. (2005) Experimental study of sliding base-isolation buildings with Magneto-rheological Dampers in near-fault earthquake. *Journal of Structural Engineering*, 131: 1025-34.

Spencer, B.F., Dyke, S.J., Sain, M.K., and Carlson, J.D. (1997) Phenomenological model of a Magnetorheological damper. *Journal of Engineering Mechanics*, 123: 230-238.

Villaverde, R. (2009) Fundamental concepts of earthquake engineering. New York: Taylor and Francis group.

Wang, Y., and Dyke, S.J. (2013) Modal-based LQG for smart base isolation system design in seismic response control. *Structural Control and Health Monitoring*, 20: 753-768.

Wongprasert, N., and Symans, M.D. (2005) Experimental evaluation of adaptive elstomeric base-isolated structures using variable-orifice fluid dampers. *Journal of Structural Engineering*, 131: 867-877.

Yang, J.N., Wu, J.C., Reinhorn, A.M., and Riley, M. (1996) Control of sliding-isolated buildings using sliding-mode control. *Journal of Structural Engineering*, 122: 179-186.

Yoshioka, H., Ramallo, J.C., and Spencer, B.F. (2002) Smart base isolation strategies employing Magnetorheological Dampers. *Journal of Engineering Mechanics*, 128: 540-551